Aluminum Bottle Forming Simulation with Abaqus

Kunming Mao

DASSAULT SYSTEMES SIMULIA CORP., Central Region, West Lafayette, IN, 47906, USA

Alejandro Santamaria

The Coca-Cola Company, One Coca-Cola Plaza, Atlanta, GA, 30313, USA

Abstract: This paper presents several modeling techniques for simulating and optimizing aluminum bottle forming using Abaqus/Explicit. Designing and tuning sheet-metal forming tools for aluminum bottles are quite complicated and time consuming tasks. These tasks must take into consideration a number of potential issues, such as the success rate of forming, bottle shape smoothness, bottle load capacity, sheet-metal over-thinning, and metal wrinkling. To shorten the design cycle and reduce the number of forming tool prototypes for the Coke Contour aluminum bottle, simulations with Abaqus served as virtual test grounds to provide valuable insight into the bottle's complex forming processes. Because of large deformation and contact interactions, Abaqus nonlinear capabilities were well suited for these tasks. This paper demonstrates Abaqus forming applications that helped resolve issues arising from realistic industrial forming design and production processes. Three bottle-forming simulations used to predict sheet-metal forming instability, metal over-thinning, and metal wrinkling are used to illustrate the effectiveness of numerical simulations.

Keywords: Coke bottle, sheet metal forming, forming instability, FLSD, FLD, MSFLD, surface smoothness, load capacity, die, closure system, thread forming, reverse draw forming

1. Introduction

A few years ago, The Coca-Cola Company (Coke) decided to revolutionize the beverage industry by developing a lightweight re-sealable aluminum bottle that would use the current aluminum can-making process as its base platform. The making of this bottle involved a number of forming stages, including cupping, cylinder drawing and ironing, die forming, and top-finish forming (threading and curling). Developing the related tools was complicated and time consuming, due to the extensive list of package performance requirements, the manufacturing process robustness, cost optimization, and other factors. Numerical simulations using Abaqus provided strong virtual test grounds for investigating these issues, validating design ideas, and seeking new optimized solutions.

This paper presents several simulation techniques using Abaqus to model three aluminum-bottle-forming processes:

- The cupping forming process that turns a flat sheet of aluminum blank into a cup shape

- The die necking and expansion processes that transforms a cylinder into the iconic Coke Contour shape

- The top-finish forming process

Although not presented here in detail, numerical simulations have also been used to investigate a number of other design and optimization issues, such as sheet-metal selection, bottle-forming visual surface discontinuities, formed bottle top-loading capacity, sheet-metal thickness optimization, and top-finish formation speed optimization. These simulations have provided information that is not easily or economically achieved in a physical test lab. They have also proven to be powerful complements to the physical lab tests.

The first step of the bottle-making process is cupping, where a blank cut from a rolled-flat aluminum sheet is drawn into a cup. The cup for aluminum bottles is dimensionally unique and requires an additional forming step not typically used when making cups for regular cans. Metal wrinkling and over-thinning were two undesirable phenomena experienced during the initial prototyping of the Contour bottle. Abaqus/Explicit simulation was able to mimic the wrinkling observed in the real world, allowing the design team to identify key setup parameters and tooling design changes to prevent wrinkling and over-thinning.

Die necking is a well-known technique used to reduce the diameter of aluminum cylinders at high speeds, but its application has been limited to the top 10 centimeters of the metal cylinder being shaped due to physical limitations of commercially available machines. Coke, in partnership with its suppliers, worked to bring longer stroke die-necking machines from other industries to the beverage landscape and broke the 10 centimeter threshold, creating the opportunity to produce previously unattainable metal packaging shapes. The resulting forming process allowed Coke to produce the iconic Contour shape with one of the most vastly used packaging materials: aluminum.

Abaqus sheet-metal forming instability prediction capability (SIMULIA, June 2008) provided extremely valuable insights after an unacceptable rate of sheet-metal fractures was observed during the bottle's initial prototyping process. Simulations were used to optimize tooling geometries and forming steps as well as to compare material selections in order to improve forming success rates.

Because of the relatively large amount of metal displacement required to achieve the shape of the bottle's upper portion, the top die-necking process can cause some small visible surface discontinuities, referred to as witness rings, which were categorized as unacceptable by Coke's marketing team. The simulations were effective for optimizing the die-necking tool profiles to alleviate the witness rings.

The bottle's column load resistance, or top-loading capacity, was another concern during the bottle-shape design. Simulations were also used to predict the top-loading capacity of the formed bottle, which led to selection of the initial sheet-metal thickness during the design stage. This ensured that the final bottle had enough strength to withstand the required capping axial loads without overusing material.

During the bottle's top-finish forming process, metal over-thinning was observed in physical tests. Simulations of the top-finish forming process reproduced the over-thinning phenomenon and provided a means to evaluate and optimize the tooling parameters required to prevent this defect.

The following sections describe how Abaqus/Explicit simulations were applied to aluminum bottle-forming processes. These simulations focus on sheet-metal forming instability prediction during the bottle necking and expansion, sheet-metal over-thinning during top forming, and wrinkling during cupping. Along with other simulations not presented here, these simulations convinced the Coca-Cola Global Packaging team that Abaqus simulations were the best tool for providing fast turn-around of design iterations, quick validation of new ideas, and reduction of costly physical tooling prototyping.

2. Sheet Metal Instability from Bottle Necking and Expansion

Die-necking and expansion are key forming processes used to turn a cylindrical aluminum shape into the iconic Coke Contour bottle shape shown on the right in Figure 1. The entire forming process consists of the three stages shown in Figure 2: deep necking, expansion, and top necking. Each of these stages consists of multiple steps that create the gradual and smooth diameter changes along the length of the bottle. The deep-necking stage can consist of up to six successive applications of die-necking processes. The expansion stage can include another six steps, and top necking can consist of as many as 30 successive insertions of die-necking tools.

A common problem during sheet-metal forming is sheet-metal necking instability. The forming process, particularly during the expansion process, can cause the sheet metal to stretch and thin, which can make the sheet metal lose its load-carrying capacity and consequently result in failure. During early stages of the prototyping process, sheet-metal splitting was observed due to sheet-metal necking instability.
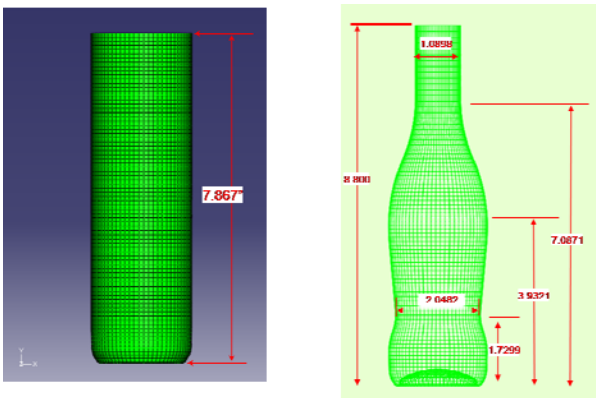

Figure 1. Forming a cylinder into a Coke Contour bottle shape by die necking and expansion.
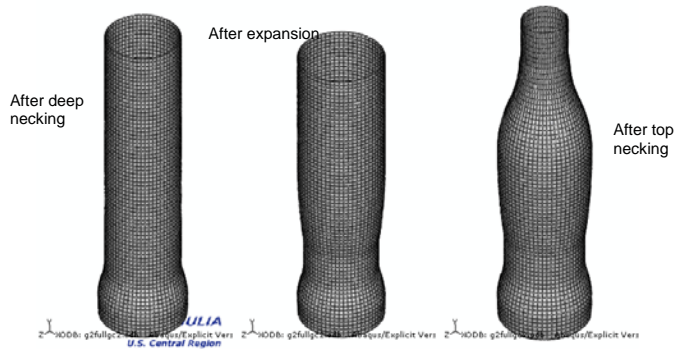
Figure 2. Intermediate shapes after deep necking, expansion, and top necking.

Sheet-metal forming instability is typically analyzed using the strain-based forming limit diagram (FLD). The FLD monitors the strain history during a forming process with respect to the sheet-metal FLD criterion, which is obtained by determining the strain-history-dependent limit strains of a number of differently shaped specimens using a dome test apparatus. Figure 3 shows test specimens used to determine limit strains for aluminum sheet metals. Figure 4 shows an example FLD.
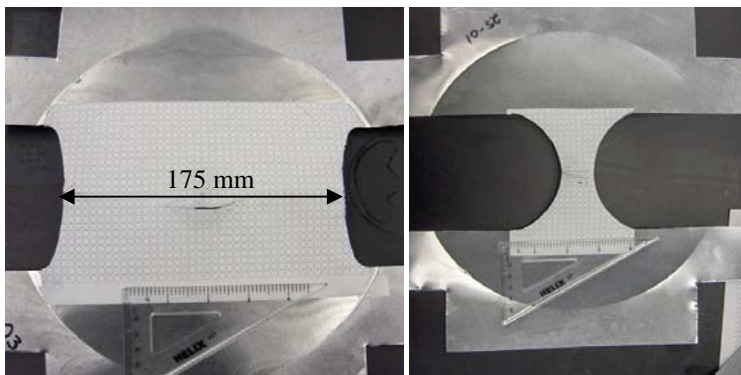
Figure 3. Test specimens used to determine limit strains.
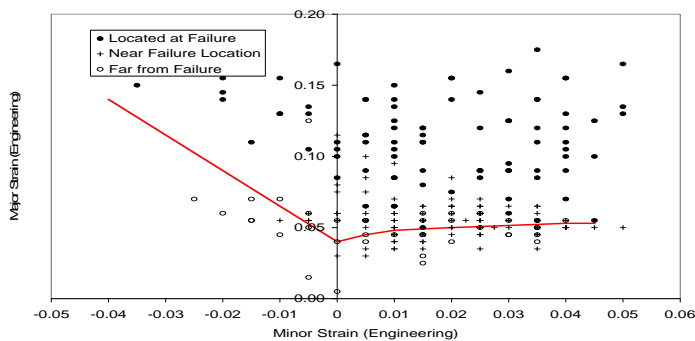
Figure 4. Forming Limit Diagram (FLD) from the dome apparatus tests

However, the FLD criterion is sensitive to the strain history. Because loading and unloading occurs repeatedly during the deep-necking and expansion stages, the strain-based FLD is not applicable in the forming of the Coke Contour bottle.

Another popular failure criterion less sensitive to the loading history is the Müschenborn-Sonne forming limited diagram (MSFLD) (Müschenborn and Sonne 1975), which predicts failure using the effective accumulative plastic strain versus the ratio of principal strain rate. However, this criterion was also not applicable, since the sheet metal underwent compression during the deep necking stage and was subject to tension during the expansion stage. The effective plastic-strain formula used in the MSFLD criterion does not distinguish the compressive strain from tensile strain, which in turn would over-predict the MSFLD criterion value for failure prediction of the bottle forming.

In contrast, the stress-based forming limit diagram (FLSD) (Sakash 2006) was less sensitive to the loading history and proved to be the best choice of the three criteria for the bottle forming problems. Table 1 illustrates the differences between these three criteria when applied to one bottle forming process, with respect to two different aluminum alloy materials. This data shows that the FLSD criterion provides the most meaningful results (close to unity) at the end of the expansion stage. As a result, the FLSD criterion was used in the Abaqus simulations for the sheet-metal forming instability prediction and the forming tooling optimization.

Table 1. Three forming-limit criteria applied to one bottle forming process.

	Max FLSD criterion value at the end of bottle expansion	Max MSFLD criterion value at the end of bottle expansion	Max FLD criterion value at the end of bottle expansion
Aluminum Alloy 1	0.954	3.567	0.191
Aluminum Alloy 2	0.991	2.618	0.333

Rolled aluminum sheet metals typically exhibit anisotropy. However, tests of the Aluminum Alloy sheet metal used in the simulations showed minor anisotropic behaviors. Figure 5 shows the 0-degree (rolling direction) and 90-degree stress-strain for the Aluminum Alloy sheet metal. Since the anisotropy was minor, the von Mises plastic theory was used after the yielding. This simplification also eliminated the need to find the local directions in the aluminum cylinder material, which was slightly different from the original sheet metal used in the material property tests, since the aluminum cylinder was formed from the original sheet metal through a number of forming processes, such as cupping.

Also shown in Figure 5 is the associated FLSD stress criterion curve for the Aluminum Alloy sheet metal. Note that the stress-based FLSD criterion was derived from the corresponding strain-based FLD criterion and the derivation calculation used the same material properties that were used in the simulation.
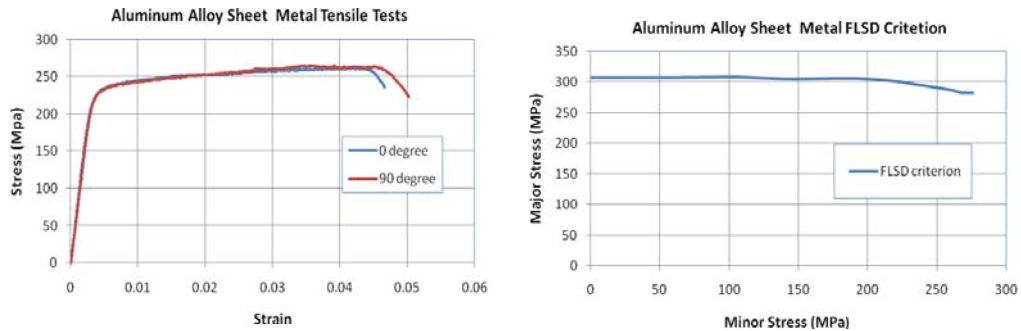
Figure 5. Stress-strain curves for the Aluminum Alloy used, and its FLSD criterion.

Abaqus/Explicit was used to simulate the bottle-forming process using the FLSD criterion and the models shown in Figure 6. As in the real forming process, the aluminum cylinder in the model is repeatedly pushed from one die to another, which gradually changes its diameter at different heights and transforms the sheet-metal cylinder model into the Coke Contour shape. The FLSD criterion used was automatically calculated during the simulations.
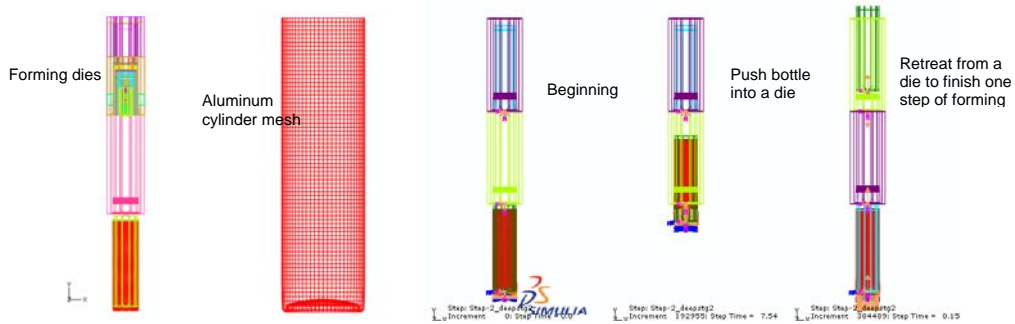
Figure 6. The finite element model, including bottle cylinder and all needed dies.

Figure 7 shows the resulting FLSD criterion values at the end of deep necking, expansion, and top necking. The FLSD criterion theory sets unity as the onset of instability. At the end of the expansion stage, the FLSD reaches the maximum value. This reflects the fact that the FLSD (or FLD) is primarily for tensile stretch instability. The expansion stage causes the sheet metal to stretch. Consequently, it contributes most to the maximum FLSD, which is the deciding factor for instability. Figure 7 also shows that the maximum FLSD criterion value barely changes during the top-necking stage. This is reasonable, since the top-necking stage is primarily a compression process.
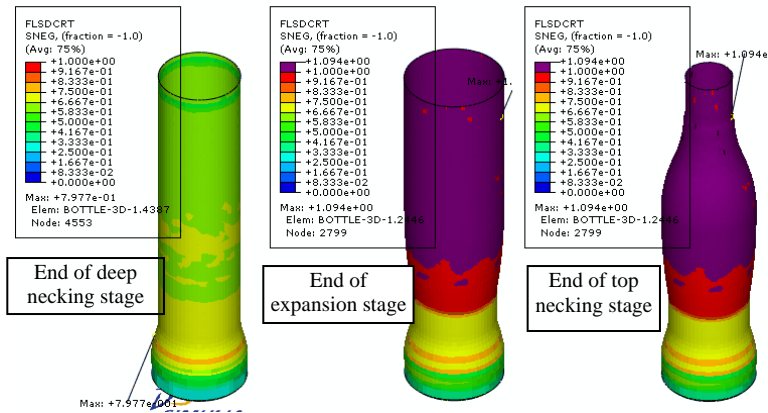
Figure 7. FLSD criterion values at the end of deep necking, expansion, and top necking.

It is important to note that failure in the real world is a complex phenomenon; the theory always includes assumptions; and the test data supporting the theory include inevitable errors, which means that there is no definite clear-cut threshold between failure and non-failure. A condition with an FLSD criterion value near or above unity only indicates that failure is likely. The analysis results must be compared with real-world observations to form a meaningful conclusion.

Using the FLSD criterion in Abaqus, the forming simulations were applied to a number of tooling profiles for different bottle configurations to search for successful solutions. The simulation shown in Figure 8 studied the effect of waist size on the maximum FLSD. Three different bottle waist reductions were studied: 15 percent, 11 percent and 8.5 percent. The corresponding maximum FLSD criterion values were 1.029, 0.994, and 0.979, respectively. The observations from the real field tests showed that the successful rates of forming were 30 percent, 86 percent, and 94 percent, respectively. This comparison provided a very good statistical correlation, which provided convincing evidence that the forming simulation, along with the FLSD criterion, was an effective tool for predicting sheet-metal instability.
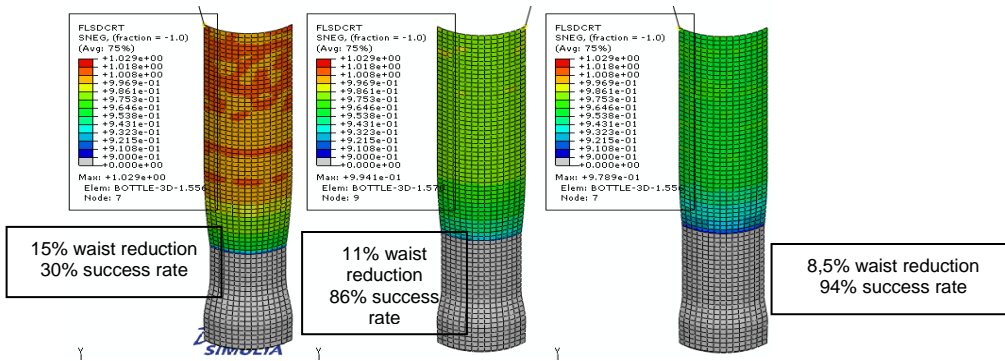

Figure 8. Effect of three waist sizes on maximum FLSD criterion.

3. Top-Finish Forming Simulation

The top-finish forming process chosen for this program consisted of the five operations shown in Figure 9: tamper-band forming, threading, pre-curling, trimming, and curling.

Figure 9. Top-finish forming operations: tamper-band forming, threading, pre-curling, trimming, and curling

Abaqus/Explicit was used to simulate the first three operations, since the focus was to study an excessive thinning phenomenon observed during the pre-curling operation. To effectively predict the failure condition of the pre-curling operation, the tamper band and the threading operations had to be included in the simulation to guarantee that the correct conditions were established. Figure 10 shows the finite element model setup.
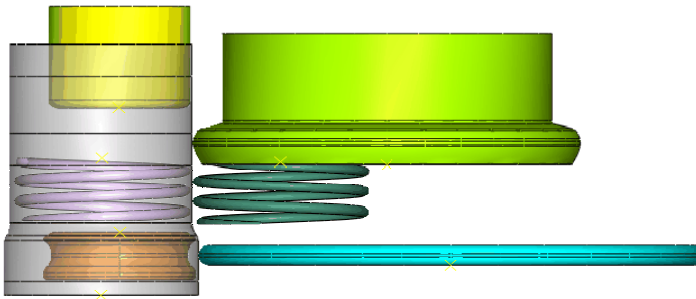
Figure 10. The finite element model for tamper-band forming, threading, and pre-curling.

To reduce the computational cost, only necessary tool geometry features were retained in the model. Similarly, only the top portion of the unformed bottle was included in the model for the top-finish forming simulation. The aluminum bottle section to be formed was modeled with S4R shell elements. All the tooling portions were defined with rigid bodies, either an analytical rigid surface or a rigid-body constraint on surface elements. The bottle model had boundary conditions at the bottom with the prescribed rotational velocity. Three sets of tools (OP1, tamper-band forming; OP2, threading; and OP3, pre-curling) were engaged in sequence in a controlled manner. The actual physical forming process took about 4.5 seconds, which was too long for the simulation. To reduce simulation duration and computing time, the bottle rotational velocity was increased in the simulation. Mass scaling was also applied. Studies were performed to verify that these speed-up measures would not impact the simulation results. Figure 11 shows the bottle mesh with approximately 10,000 elements for the top portion of the bottle, the geometries for the inner

and outer thread-forming die pairs used in OP2, and their simplified finite element representation. As illustrated in the figure, only the spiral snake-like thread portion was used in the finite element model, since only these surfaces contacted the sheet metal, given the fact that the tooling geometries still consume computational resources despite their rigid-body representation. Figure 12 illustrates the intended engagements of the tools during the OP1, OP2 and OP3 forming stages.
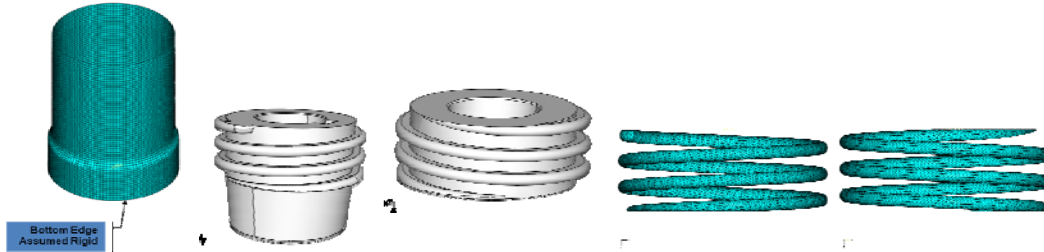

Figure 11. Bottle mesh, OP2 threading-forming die geometries, and their finite element representations.
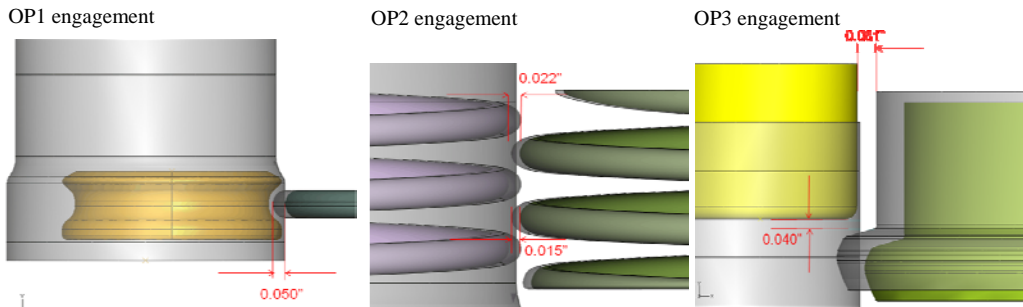
Figure 12. Intended tool engagements during OP1, OP2, and OP3 forming stages.

The simulation used a heat-treated aluminum sheet metal, whose stress-strain curve is shown in Figure 13. Note that the material curve used a constant-slope extrapolation (pink curve) at the end of test data, in order to prevent excessive deformation due to the default constant-value extrapolation.
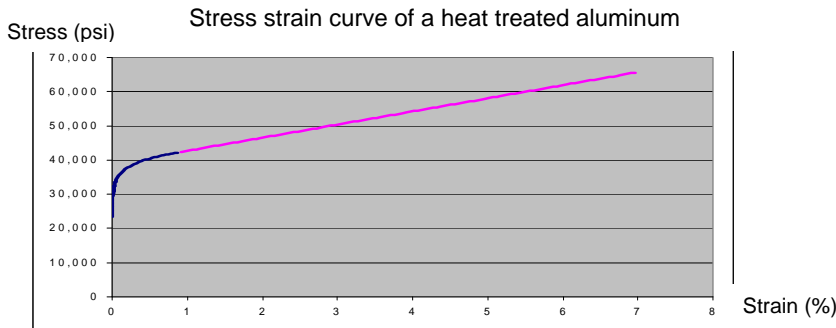

Figure 13. Heat-treated aluminum sheet-metal material curve used in analysis.
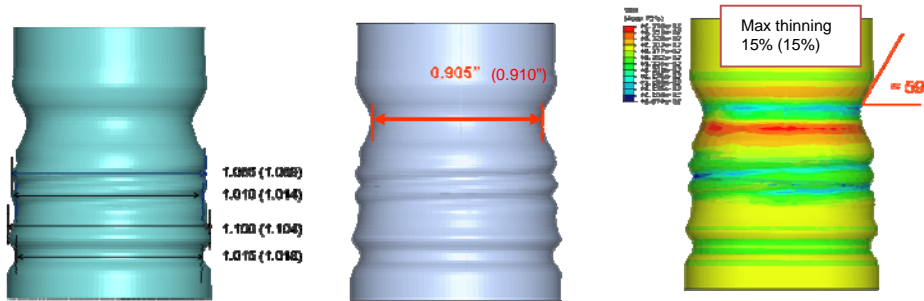
Figure 14. Simulation results as compared to the field-measured data (in parenthesis).

The results from the simulation of a 0.013-inch gage aluminum sheet metal were compared with the field-measured data shown in parenthesis in Figure 14. The simulation provided a very accurate prediction of maximum thinning (15 percent) seen in the real world and validated the simulation techniques for future numerical virtual tests, which could be used to fine tune parameters used to optimize the production line.

4.   Cupping Simulation

The forming process for making the cup is called draw-reverse-draw, which bends the blank into a smaller diameter cup in two steps. In the first step, tools engage the blank to draw an initial cup. In the second step, a different set of tools turn the initial cup inside-out. During the initial prototyping, the finished cups showed unacceptable amounts of wrinkling, as shown in Figure 15. The intuitive solution to alleviate wrinkles was to increase the metal hold-down pressure, which would also increase the gripping shear force to the sheet metal, but this could cause side-wall thinning.

Figure 15. Wrinkling in half-formed cup (left, right) and satisfactory cup (middle).

Abaqus/Explicit simulated the real-life cup forming process by replicating the wrinkling and thinning observed in the real world. Consequently, it paved the way to study the effects of adjustable parameters through simulation, as well as modify the tool geometries as necessary.

Figure 16 shows the tooling die set assembly with all relevant pieces. Figure 17 illustrates the draw-reverse-draw cup-forming process. The green element in the diagram represents a segment (slice) of the aluminum blank. The forming sequence starts with the blank and draw pushing down the blank, with the lower pressure pad (LPP) holding down the aluminum blank on its outer region. The downward movement of both blank and draw and lower pressure pad draw the initial cup. The final cup is formed as the draw punch pushes the center of the initial cup and turns it inside out. During this forming sequence, the cup's sidewall experiences thickening and thinning. Figure 18 shows the cup's wall-thickness distribution measured along the cup's height after the full forming sequence, starting with the initial metal blank gauge reading of 0.0140 inches.
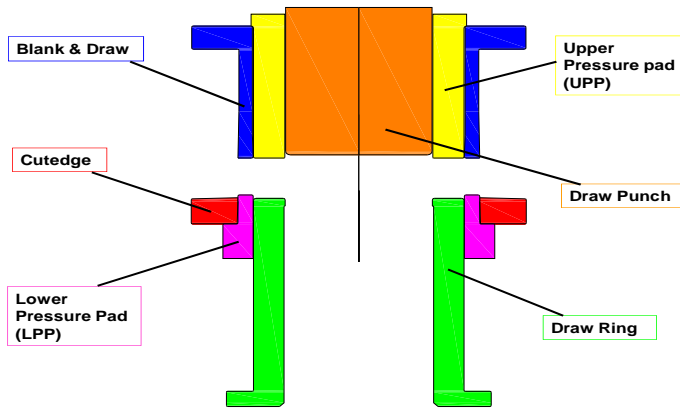

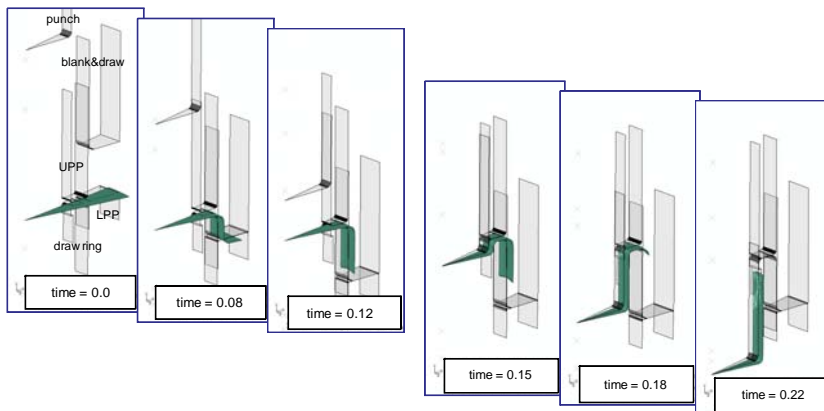**Figure 16. Cross-section view of cupping tooling diagram.**

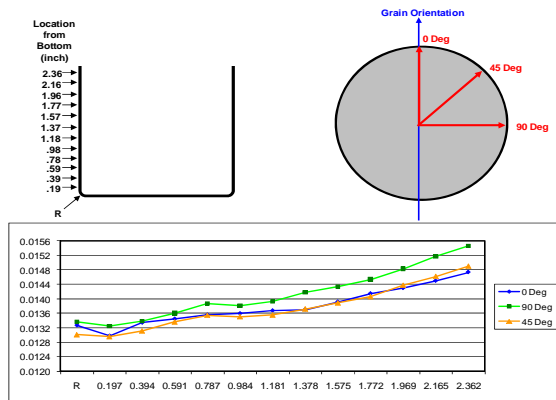**Figure 17. Sequence of draw-reverse-draw cup-forming process.**

Figure 18. Measured distribution of thickness along the height after cup forming.

Studies were performed to determine appropriate modeling dimensions and indicated that a 15-degree segment of blank sheet metal with approriate boundary and loading conditions was sufficient to understand the wrinkling and thinning phenomena due to the symmetrical nature of the final cup. This provided high modeling efficiency and fast study turn-around time. Figure 19 shows the mesh using S4R shell elements for the 15-degree segment blank finite element model. All tooling profiles were modeled with analytical rigid surfaces. Movements of all tool components were either controlled according to the real tooling conditons or driven through contact with other components. Connector elements were used to provide necessary stops and damping to reflect the real machine mechanism. The lower and upper pressure pads featured load control to represent the pneumatic pressure control used in real life. A necessary mass effect was included in the model.
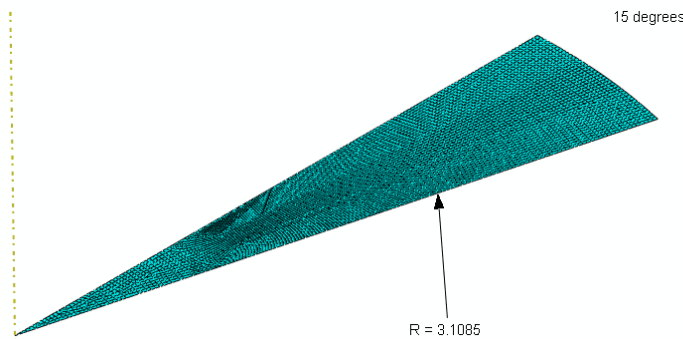

Figure 19. A15-degree segment of the finite element mesh using S4R shell elements.

The Abaqus/Explicit simulations duplicated the wrinkling and thinning seen in real life. Figure 20 shows the out-of-plane plastic strain contour and deformation plots, which clearly indicate the wrinkling. The wrinkling occurs when the final cup is drawn as the draw punch pushes down the metal blank during the second step of the draw-reverse-draw process.
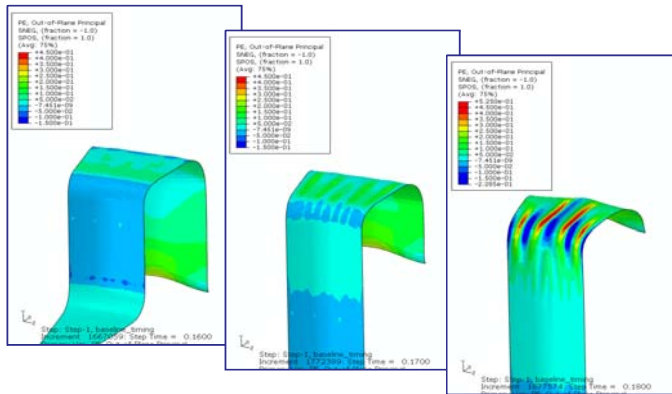
Figure 20. Wrinkling revealed by Abaqus/Explicit simulations.

The simulations also duplicated the thinning. Figure 21 shows the thickness-distribution profile for the cup and shows that the thickness varies after forming from the initial 0.014-inch thickness. Figure 21 also shows a comparison between the simulation results and the real measurement. Note that the difference between the real measurement and the prediction in the thinnest region is about one percent, which could be attributed to unknowns or unaccounted parameters such as friction and pneumatic pressure. However, the trends from the simulation and the real measurement were very close, which was sufficient for process optimization.
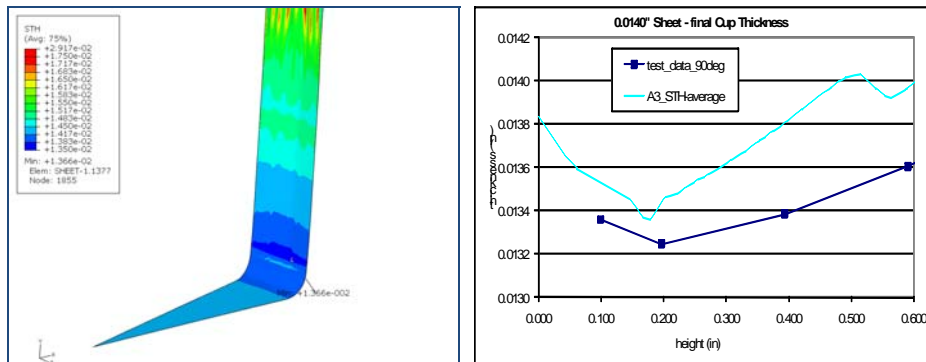

Figure 21. Thickness distribution after forming and comparison with real measurement.

After the initial correlations, the focus was shifted to the investigation of tool geometry and design parameter changes using Design of Experiments (DOE) approaches. Key factorials were identified and simulated as shown in Figure 22. Two configurations were used: a flat upper pressure pad (UPP) configuration and a contoured UPP configuration. The contoured UPP configuration had an additional radius of R2 in the corner of the UPP. One key change was to vary the radius R1 in the corner of the drawing ring, and the other was to change the UPP corner radius R2. Across the three variations of R1, A1, A3, and A5, the radius R1 increased from A1 to A5, with A3 being the base configuration. Similarly, for the three categories of the contoured UPP corner radius R2, B, D, and F, the radius was also in ascending order from B to F.
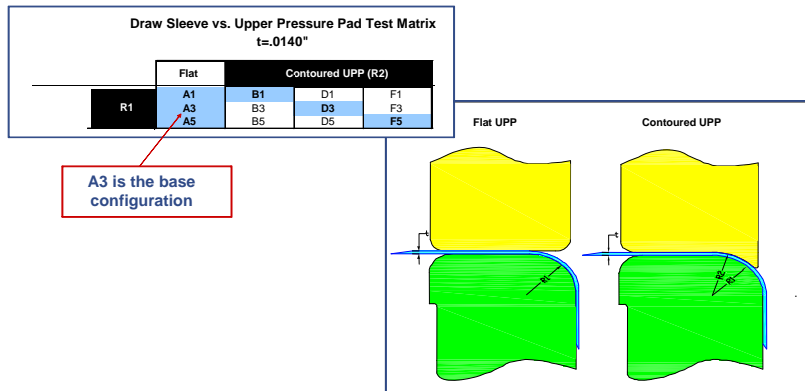
Figure 22. Key factorials in the DOE study.

Figure 23 shows the deformed shapes from the simulations. Factorial A1 and factorial B1 provided improved results for wrinkling prevention, as did factorials D3 and F5. The reduction of wrinkling was attributed to the increased metal tension and structural stiffness induced by the tighter turning radius on the corner of the draw ring. The contoured UPP corner provided additional holding surface area that increased the stiffness and metal tension and further prevented wrinkling. However, the simulations also suggested that the use of combined countermeasures, reducing the corner radius and using the contoured UPP corner, did not deliver additional benefits.
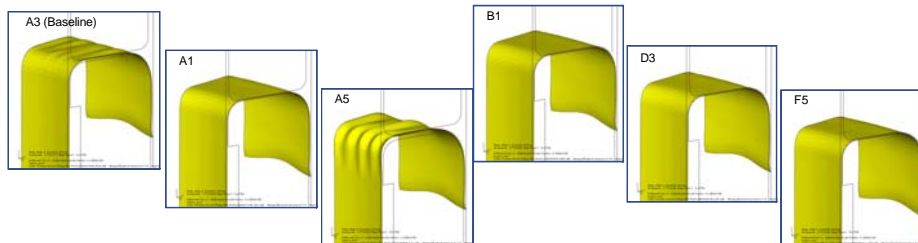

Figure 23. Forming results from DOE studies.

One additional benefit of the cup-forming simulations was information on how thinning was related to friction and pressures on the UPP. The investigation showed that there was a delicate balance among the pressure on the UPP and thinning and wrinkling. Specifically, higher pressure on the UPP could be useful for suppressing wrinkling. However, the higher pressure could also cause more frictional gripping force on the sheet metal, which could make the draw-punch tool cause too much sheet-metal thinning during the reverse-draw process. This kind of delicate relationship also emphasized the importance and benefit of the numerical simulations.

5. Conclusions

The techniques and examples presented in this paper clearly demonstrated that Abaqus/Explicit was a useful tool for expediting and optimizing many kinds of metal package-forming processes.

The project work discussed here successfully addressed in a timely manner a number of real-world issues, such as the necessity for a high success rate during the forming process, predictable load-carrying capacity, and good surface aesthetics. To achieve these goals in the face of time-consuming and costly tool redesign and test processes, numerical simulations with Abaqus were powerful virtual test grounds that modeled the actual forming process and incorporated needed theories, like stress-based forming limit diagrams (FLSD). Additionally, the numerical simulations for the three cases presented in this paper correlated very well with physical test results.

Most of the solutions developed through Abaqus/Explicit simulations were implemented on a bottle pilot production line, resulting in the reduction of the package's development time of about 75 percent, combined with a 50 percent reduction in cost. The learning from this work is still being used in active metal-packaging projects beyond aluminum bottles and is continuing to inspire engineers at The Coca-Cola Company to innovate beyond the consumer's imagination.

6. Acknowledgements

7. References

1. Dassault Systémes Simulia Corp., 2008. "Abaqus Analysis User's Manual" (June).

2. Sakash, A., S. Moondra, and B. Kinsey, 2006. "Effect of yield criterion on numerical simulation results using a stress-based failure criterion." *Journal of Engineering Materials and Technology* 128 (July).

3. Müschenborn, W., and H. Sonne, 1975. "Influence of the Strain Path on the Forming Limits of Sheet Metal," *Archiv fur das Eisenhüttenwesen* 46, no. 9: 597–602.